

DISK AND WIND EVOLUTION OF THE FAST ROTATOR ACHERNAR.

S. Kanaan¹, A. Meilland, Ph. Stee, A. Domiciano de Souza² and D. Briot³

Abstract. We use spectral energy distributions (SEDs), H α line profiles, and visibilities available in the literature to study Achernar's envelope geometry and to propose a possible scenario for its circumstellar disk formation and dissipation. We use the SIMECA code to investigate possible geometries by comparing our synthetic results with spectroscopic and high angular resolution data from the VLTI/VINCI instrument. We compute three different kind of models : an equatorial disk, a polar wind, and a disk+wind model. We have developed a 2D axial symmetric kinematic model to study the variation of the observed H α line profiles, which clearly evidence Achernar's equatorial disk formation and dissipation between 1991 and 2002. Our model can reproduce the polar wind extension greater than $10 R_{\star}$ and a possible equatorial disk ($\leq 10 R_{\star}$) but, due to the lack of interferometric data at short baselines, we were not able to estimate the wind opening angle. We have also reproduced the H α line profiles variations using an outburst scenario but the disk final contraction needs an additional unknown physical effect to be taken into account. New interferometric observations at short baselines ($5 \leq B \leq 20$ m) are mandatory to constrain Achernar's circumstellar envelope, as well as spectroscopic long term following to link Achernar's mass loss episodes with its circumstellar disk formation.

1 Introduction

Be stars observations are clearly evidencing that these stars are variable with a variability time-scale ranging from minutes to decades (Porter & Rivinius 2003). Phase transition are revealed by Balmer line emission intensity and global line profile changes as well as changes in the visible spectral energy distribution. Variations in the emission lines can occurred over periods of years, months or even days (Porter & Rivinius 2003). These changes can be either due to variations of the physical structure and size of a more or less permanent circumstellar environment (CE), or to the creation of a new CE during mass ejection events of the central star. Interferometric and linear polarization measurements put some observational constraints on the CE flattening (Gies et al. 1990; Stee et al. 1994; Quirrenbach et al. 1997; Yudin 2001; Tycner 2004). Nevertheless, the disk formation and its geometry is still poorly known but the situation is changing rapidly with the recent CHARA (Gies et al. 2006), NPOI (Tycner et al. 2006) or VLTI interferometric measurements (Meilland et al. 2006b).

In a recent study regarding the determination of fundamental parameters for 130 Be stars, taking into account the gravitational darkening, Fremat et al. (2005) have shown that Be stars rotate on average at an angular velocity ratio $v/v_c \approx 0.88$. On the other hand, interferometric measurements of the brightest known Be star, α Eri (Achernar), carried out by Domiciano de Souza et al. (2003), suggest that this star has a flattening exceeding the predicted one assuming a critical rigid rotator Roche model.

The objective of our study is to model Achernar circumstellar envelope using the whole VLTI/VINCI data set obtained by Kervella & Domiciano de Souza (2006; hereafter KD) in order to investigate if the flattening ratio is smaller than the one they have estimated and can rather be interpreted thanks to a small circumstellar contribution.

¹ Observatoire de la Côte d'Azur- Département GEMINI - CNRS-UMR 6203 Avenue Copernic, Grasse, France

² Laboratoire Universitaire d'Astrophysique de Nice - CNRS-UMR 6525, France

³ Observatoire de Paris, 61, Avenue de l'Observatoire, 75014 Paris, France.

2 Achernar

The star Achernar (α Eridani, HD 10144) is the nearest ($d = 44$ pc, Hipparcos) and brightest ($V = 0.46$ mag) of all Be stars. Depending on the author (and the technique used) the spectral type of Achernar ranges from B3-B4IIIe to B4Ve (e.g. Slettebak 1982, Balona et al. 1987).

The estimated projected rotational velocity $v \sin i$ ranges from 220 to 270 km/s and the effective temperature T_{eff} from 15000 to 20000 K (e.g., Rivinius *priv.comm.*, Chauville et al. 2001, Vinicius et al. 2005). Achernar rapid rotation ($\geq 80\%$ of its critical velocity) induces mainly two effects on the stellar structure: a rotational flattening and a gravity darkening described by the Von Zeipel effect (Von Zeipel 1924).

Achernar rotational flattening was measured for the first time by Domiciano de Souza et al. (2003) using the VLTI and its testbed instrument VINCI. The measured flattening ratio is $R_{eq}/R_{pole} \approx 1.5$.

On the other hand Vinicius et al. (2005) have evidenced, following $H\alpha$ line profiles variations, a circumstellar disk contribution instead of a purely flattening photosphere. Thus, KD reprocess the whole visibility VINCI data set with a rather complete (u,v) plane coverage to see if it might be possible to evidence an equatorial or a polar extension. Following this study, they were able to evidence a polar extension rather than an equatorial disk.

3 SIMECA: a code dedicated to active hot stars

The SIMECA code computes classical observables, i.e. spectroscopic and photometric ones, but also intensity maps in Hydrogen lines and in the continuum, in order to obtain theoretical visibility curves that can be directly compared to high angular resolution data. The main hypothesis of this code is that the envelope is axi-symmetric with respect to the rotational axis. No meridian circulation is allowed. It is assumed that the physics of the polar regions is well represented by a CAK type stellar wind model (Castor et al. 1975) and the solutions for all stellar latitudes were obtained by introducing a parametrized model that is constrained by spectrally resolved interferometric data. The inner equatorial region is dominated by Keplerian rotation. The basic equations of the SIMECA code are given in details in Stee & Araújo 1994.

We have modified the original code in order to simulate Achernar stellar surface and its circumstellar environment. Since it is the nearest Be star (44 pc) and because its circumstellar environment should not be very extended ($\leq 30R_*$), we have refined the computed grid around the central star and decrease the maximum possible extension of the envelope, which can reach up to 100 R_* in the original version. We have also suppressed the continuum opacity computation since the envelope is supposed to be optically thin at $2 \mu\text{m}$ which drastically decrease the computation time by a factor 10.

The main modification done was to take into account Achernar's photosphere deformation as well as the Von Zeipel effect. Since the original SIMECA code assumed spherical stars with uniform T_{eff} we have introduced, in this new version, an elliptical star ($R(\theta)$) according to:

$$R(\theta) = R_{pole} R_{eq} (R_{pole}^2 \cos^2(\theta) + R_{eq}^2 \sin^2(\theta))^{-1/2} \quad (3.1)$$

and introduce a gravitational darkening law ($T_{eff}(\theta)$)

4 Disk and/or wind scenario ?

Vinicius et al. (2005) have evidenced a CE using Achernar $H\alpha$ line profile observed from 1991 to 2002. Since the 1999 line profile exhibits a maximum absorption, they used it as the "true" stellar photospheric absorption profile and subtracted it from all remaining $H\alpha$ lines observed. The $H\alpha$ line components obtained reveal residual emission. This residual emission was interpreted by Vinicius et al. as caused by an equatorial disk and they put forward the dissipation of the disk between 1993 and 2000 and its actual formation. Nevertheless, Achernar's SED does not exhibit any IR excess compared to a classical Be star which puts strong constraints on the CE density distribution which must remain very small.

KD analyze the whole visibility data set of Achernar showing that the distribution of the measured visibility around the pole does not follow a uniform disk. There is a clear "switch-off" of the visibility at small baselines that KD interpreted as a polar wind signature.

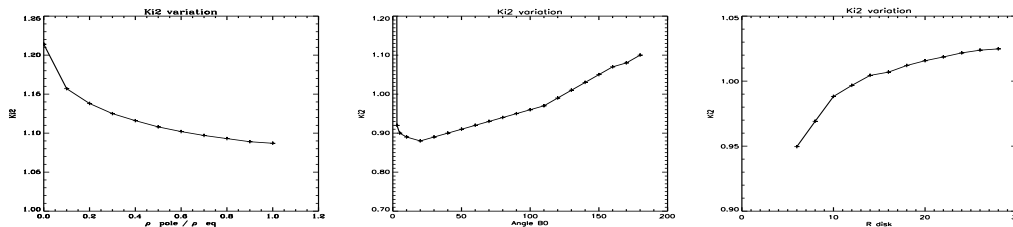


Fig. 1. (left) χ^2 values obtained for a disk model decreasing when going from a thin equatorial disk to a more spherical circumstellar envelope, (center) χ^2 values obtained for a wind model showing a minimum value for an opening angle around 20° , (right) χ^2 values obtained for a wind+disk model as a function of the equatorial disk radial extension in stellar radius.

On the other hand it is not clear if there is an equatorial extension from their data since there is no clear "switch-off" in the equatorial direction whereas a clearer signal is seen along the polar axis. Finally they concluded that the VLTI/VINCI data of Achernar is compatible with a flattened star with a polar wind.

To further investigate these issues concerning the disc and/or wind around Achernar, a complete astrophysical model able to simultaneously explain all spectroscopic and interferometric observations is required.

In order to test the scenario proposed by KD, we compute the visibilities and the corresponding χ^2 for three different kind of models using the SIMECA code:

1) A disk-like envelope model. In this scenario we run more than one hundred different models with different opening angle, densities and various disk parameters without been able to fully agree with the observed VLTI/VINCI data. Thus, we were forced to exclude this first scenario for the epoch of the VINCI observations. We obtained $\chi^2 \geq 1$ for all our disk-like models as seen Fig. 1. Since the VLTI/VINCI data clearly evidence a polar wind contribution the χ^2 are decreasing when considering a pure equatorial thin disk to a more spherical circumstellar geometry which mimics a stellar wind contribution along the polar axis. Globally the χ^2 obtained are larger for these models compared to the pure wind model presented in the following item.

2) A polar wind model. The visibilities computed with SIMECA for several wind models with different opening angle are in good agreement with the observed VLTI/VINCI data. The χ^2 values obtained for our best models are less than 1.0 with a minimum of 0.88 for an opening angle around 20° (see Fig.1). Thus, a distorted central star with a polar wind seems to be a possible scenario for Achernar as proposed by KD.

3) A disk+wind scenario. The visibilities computed with SIMECA for our best models obtained are also in agreement with the VLTI/VINCI data and the corresponding χ^2 in Fig.1. As expected, the χ^2 is decreasing for a decreasing equatorial disk size but stay larger than the minimum value obtained for the wind model only (0.88). We were not able to obtain solutions for disk sizes smaller than 5 stellar radii due to numerical instabilities with the SIMCA code. Nevertheless, extrapolating the curve from Fig.1 we obtain a $\chi^2 \simeq 0.9$ for disk with $1 R_\star$ in size, i.e. again larger than those obtained for the wind scenario.

For the 3 scenarios presented we keep the flux ratio between the disk, wind, disk+wind and the central star close to 5 %. Thanks to this study we can clearly exclude the disk model but the situation is not as clear between the polar wind and the disk+wind scenarios if, for the latter case, the disk is smaller than $10R_\star$. On the other side, we obtain that Achernar's polar extension must be larger than $10R_\star$ to fully fit the interferometric data and the minimum χ^2 obtained was for the wind scenario only. Note that since there is more or less no IR excess the SED, which is dominated by the central star emission, is similar for all the models presented in this paper. Thus at the time of the VINCI observation Achernar seems to have no equatorial disk but rather a confined polar stellar wind with a $\sim 20^\circ$ of opening angle. Nevertheless, we must admit that due to the lack of interferometric measurements at small baselines this wind opening angle must be taken cautiously since it comes from our modeling but is not constrained by the VINCI data.

5 Evidence of an equatorial disk formation and dissipation

5.1 Spectroscopic data

Vinicius et al. (2005) present $H\alpha$ spectroscopic observations between 1991 and 2002. This line was almost always in absorption, but has also shown strong morphological and equivalent width (EW) variations. These variations can be related to a modification of a weak circumstellar envelope emission. They determined that there was almost no emission in 1999, and that the $H\alpha$ line profile observed at this time corresponded to the stellar photospheric absorption line. By subtracting this 1999 profile to other line profiles they obtained the residual emission profiles for all measurements between 1991 and 2002.

All emission line profiles are strongly double peaked (except for 1999 and 2000) and the double peaks separation (DPS) vary between 210 and 450 km.s^{-1} . This double peaked structure in emission lines is usually associated with a rotating disk, however a polar wind can also produce such profile (Stee & Araújo 1994). Nevertheless, the velocities measured with the double peaks separation are not consistent with a polar wind model since terminal velocities of classical Be star are very high, about 1000km.s^{-1} . Taking an inclination angle of 50° , this would have produced DPS around 1500km.s^{-1} which is far above the upper limit of what was observed. Moreover, considering that Achernar $V \sin i$ is 230km.s^{-1} and that the putative circumstellar equatorial disk is smaller than $10R_\star$, the corresponding DPS for a rotating equatorial disk would be between 144km.s^{-1} (for a $10R_\star$ uniform disk) and 460km.s^{-1} (i.e $2V \sin i$) which is fully compatible with the measured values.

An additional evidence for the presence of a small circumstellar disk is the correlation between the line profile intensity and the DPS presented Fig. 2. When the emission is weak (i.e 1991, 1998, 2002) the DPS is very close to twice the stellar $V \sin i$ whereas when the emission is stronger (i.e. 1993, 1994, 1995) the DPS is smaller. This can be interpreted by variations of the disk global extension. Since the $H\alpha$ line profile was observed through a whole cycle of variations we propose in the following a possible scenario for the formation and the dissipation of the disk.

In Fig. 2 we plot the $H\alpha$ intensity normalized by the maximum of emission (in 1993) as a function of the DPS normalized by $2V \sin i$. We can separate the disk creation/dissipation cycle in 3 phases:

- Phase 1 : Between 1991 and 1993 the DPS decreases as the intensity increases.
- Phase 2 : Between 1993 and 1995 the intensity decreases as the DPS remains nearly constant.
- Phase 3 : Between 1995 and 1999 The DPS increases again as the intensity slowly decreases.
- Phase 1 (again) : Between 2000 and 2002. The disk is reforming but in 2002 the $H\alpha$ line profile is smaller than the 1991 one. Thus, assuming that the variation is periodic or pseudo-periodic, we can roughly estimate a pseudo cycle around 13 years, in agreement with the average emission cycles duration of 11 years obtained by Vinicius et al. (2005).

We can also estimate the disk radius by assuming that the disk is keplerian. In this case, its outer radius is given by :

$$R_{disk}/R_\star = \left(\frac{2V \sin i}{DPS}\right)^2 \quad (5.1)$$

Since at the maximum of emission (in 1993) the DPS is 211 km.s^{-1} , the corresponding disk extension is $4.8R_\star$. We have also gathered data between 1960 and 1990 from the literature : Jachek et al. 1964, Andrews et al. 1966 and Hannuschick et al. 1988, 1996. These data, presented including Vinicius et al. data, exhibit that both DPS and line intensity variation seem to be quasi-periodic, with a pseudo period between 12 and 16 years.

5.2 2D kinematical model

In order to test several hypothesis for the disk formation/dissipation processes we have developed a simple 2D axisymetric kinematical model.

We first start by setting the 1D expansion velocity field. These values can evolve in time but does not depend on any forces (i.e it is why we called it Kinematic and not Dynamic model). The 1D density distribution, $\rho(r)$,

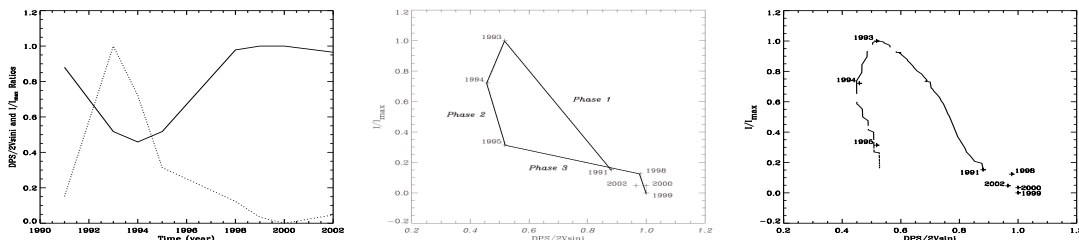


Fig. 2. (left) Solid line : H α Double Peak Separation (DPS) normalized by $2V \sin i$ plotted as a function of time for the 1991-2002 Vinicius et al. data period. Dotted line : H α line profile intensity normalized by the maximum intensity (in 1993) plotted as the function of time for the same period, (center) Normalized Intensity as a function of the normalized DPS for the 1991-2002 Vinicius et al. (2005) data period, (right) Normalized DPS / Normalized Intensity diagram for the Bursting scenario. Each solid line corresponds to one year of the evolution process. The accordance with the measurements are almost perfect for the 1991-1995 period. But this model failed to reproduce the 1995-1999 DPS variation.

is calculated for all radius using the continuity equation and with boundary conditions given by $\rho(0)=\rho_{phot}$ and $\rho(5R_{\star})=0$. This 1D density distribution is then used to create a 2D axisymmetric grid. The rotational velocity field, $v_{\phi}(r)$ is defined by :

$$v_{\phi}(r) = V_{rot} \cdot \left(\frac{r}{R_{\star}} \right)^{\beta} \quad (5.2)$$

where V_{rot} is the stellar rotational velocity and β is the exponent of the rotational velocity law. According to recent observations (Meilland et al. 2006) we have used the keplerian rotation law in our modeling ($\beta=-0.5$).

5.3 Outburst scenario

Several scenarii were tested for the formation and dissipation of the disk but the outburst scenario is the best model that can explain both phase 1 (formation) and phase 2 (dissipation almost without variation of the DPS) of the line profile variation. In this "Outburst scenario", $\phi_M(0)$ starts at its maximum and then falls to 0 as an adjustable power law. The burst propagates in the circumstellar environment forming a disk structure with a sharp outer edge (i.e. depending on the mass-flux decrease time-scale, as in the previous subsection). Such "Outburst scenario" have already been studied to explain the spectroscopic variations of some Be stars (Rivinius et al. 2002).

By adjusting the mass-flux power-law and the expansion velocity we can reproduce not only the observation of the disk formation (1991-1993) but also the beginning of the disk dissipation (1993-1995). The normalized DPS / normalized intensity diagram is plotted in Fig. 2, using a mass-flux decrease following a $t^{-0.5}$ law, an expansion velocity of 0.2km.s^{-1} and a maximum disk radius of $6R_{\star}$.

But this scenario is not totally satisfying since the phase 3 (1995-1999) is not well represented. As the intensity continue to drop the normalized DPS does not increased significantly and converge to a 0.6 value whereas the 1998 observation shows a value around 0.97. No classical dissipation scenario was able to reproduce such variation and some additional physical mechanism must be added to our model in order to reproduce it.

5.4 Contraction of the disk?

The phase 3 (between 1995 and 1999) is a major problem in the modelling of Achernar equatorial disk formation and dissipation since the DPS rising between 1995 and 1999 cannot be reproduced using a simple slowly expanding model. In fact a possible explanation may be a disk contraction with a slow decrease of density. However this phase is still an open question.

6 Conclusion

We have used the SIMECA code based on a physical model in order to interpret the VINCI data from KD who rather used a simple model by assuming a 2D elliptical Gaussian envelope superimposed on a uniform ellipse for

the central distorted star. We evidence a clear polar wind with a 5% contribution to the total flux and a spatial extension greater than $10 R_*$ in agreement with the results obtained by KD. We also conclude that at the time of the VINCI observations Achernar seems to have no equatorial disk but rather a confined polar stellar wind with a poorly constrained $\sim 20^\circ$ of opening angle.

The stellar and disk parameters used in this study are compatible with those obtained in Vinicius et al. (2005), i.e. same photospheric density of $6.3 \cdot 10^{11}$ and roughly the same effective temperature, i.e. 15000 K for Vinicius, whereas we have adopted a latitude dependent effective temperature ranging from 8500 K (equator) to 20000 K (pole). The plot in Vinicius et al. (2005) Fig. 14 showing the specific intensity at the equator as a function of the disk radial extension $< 3 R_*$ is also compatible with our finding of a wind+disk scenario with a disk $< 5 R_*$ since we are lacking of interferometric data at small baselines to strongly constrain the disk size. Nevertheless, our results strongly disagree with the disk/star flux ratio of 27 % in Vinicius whereas we obtain a value < 5 %. Using a value of 27 % would have produced visibilities out of the VINCI measurements.

On the other hand the study of Achernar's spectroscopic data between 1991 and 2002 made by Vinicius et al. (2005) evidenced an equatorial disk. Thus, we have used these $H\alpha$ line profiles to study their variations and found a clear signature of the formation-dissipation of the equatorial disk. The disk evolution follows 3 phases, the first two were reproduced with an outburst scenario whereas we need another (unknown) physical effect to explain the third phase corresponding to the final contraction of the disk. As already outlined in KD, it seems that the polar wind may be present independently of the phase of the central star (B or Be phase), i.e the polar stellar wind does not seem to be linked to the presence of a disk or a ring around the star.

7 Acknowledgments

The Programme National de Physique Stellaire (PNPS) and the Institut National en Sciences de l'Univers (INSU) with the Bonus Qualité Recherche (BQR) from the Observatoire de la Côte d'Azur are acknowledged for their financial supports.

References

- Andrews P.J., & Breger M., 1966 Observatory 86,108
 Araújo, F. X., & Freitas Pacheco, J. A. 1989, MNRAS, 241, 543
 Balona, L. A., Engelbrecht, C. A., & Marang, F. 1987, MNRAS, 227, 123
 Castor, J.I, Abbott, D.C., Klein, R.I. 1975, ApJ, 195, 157
 Chauville, J., Zorec, J., Ballereau, D., et al. 2001, A&A, 378, 861
 Domiciano de Souza, A., Kervella, P., Jankov, S., et al. 2003, A&A, 407, L47
 Fremat, Y., Zorec, J., Hubert, A.M., & Floquet, M. 2005, A&A, 440, 305
 Gies, D. R., McKibben, W. P., Kelton, P. W., Opal, C. B., & Sawyer, S., 1990, AJ, 100, 1601
 Gies, D. R., Bagnuolo Jr., W.G., Baines, E.K. et al. 2006, ApJ, submitted
 Hubeny, I. 1988, Computer Physics Comm, 52, 103
 Hubeny, I. & Lanz, T. 1995, ApJ, 439, 875
 Kervella P. & Domiciano de Souza, A. (KD) 2006, A&A, 453, 1059
 Meilland, A., Stee, P., Zorec, J., Kanaan, S. 2006a, A&A, astro-ph/0606233
 Meilland, A., Stee, Ph., Vannier, M. et al. 2006b, A&A, astro-ph/0606404
 Porter, J. M., & Rivinius, T. 2003, PASP, 115, 1153
 Quirrenbach, A., Bjorkman, K.S., Bjorkman, J.E., et al. 1997, ApJ, 479, 477
 Slettebak, A. 1982, ApJ, 50, 55
 Stee, Ph., & Araújo, F.X. 1994, A&A, 292, 221
 Stee, Ph., Araújo, F.X., Vakili, F. et al. 1995, A&A, 300, 219
 Stee, Ph. & Bittar, J. 2001, A&A, 367, 532
 Stee, Ph. 2003, A&A, 403, 1023
 Tycner, Ch. 2004, PhD Thesis, University of Toronto
 Tycner, Ch., Gilbreath G.C., Zavala, R.T. et al. 2006, AJ, 131, 2710
 Vinicius, M.M.F., Zorec, J., Leister, N.V., & Levenhagen, R.S. 2005, A&A, 446, 643
 Von Zeipel, H. 1924, MNRAS 84, 665
 Yudin, R. V. 2001, A&A, 368, 912